

Day Ahead Optimal Scheduling of Smart Community Microgrid Based on Improved NSGA-III

Meixuan ZHAO^a, Xueli HAO^{a,b}, Lili PEI^{c,1}, Hangying LI^a and Wei LI^a

^a *School of Information Engineering, Chang'an University, Xi'an, China*

^b *Anhui Key Laboratory of Intelligent Transportation, Anhui Keli Information Industry Co., Ltd., He'fei, China*

^c *School of Data Science and Artificial Intelligence, Chang'an University, Xi'an, China*

Abstract. Urban Microgrids have complex topologies and operating environments. This leads to extreme volatility and instability when high percentage of renewable energy is integrated into them. To address these problems, we propose a day-ahead optimal scheduling model for the smart community microgrid on the basis of the improved non-dominated sorting genetic algorithm III (NSGA-III). It minimizes the day-ahead operating cost of the microgrid while balancing electricity load. Firstly, we design a wind/solar/hydrogen storage self-consistent energy system inside the community microgrid to realize the efficient utilization of renewable energy. Secondly, we introduce an adaptive mutation-crossover strategy, and propose a fuzzy inference-based NSGA-III algorithm, to solve the slow convergence speed and poor convergence stability of the current multi-objective optimization algorithms. Finally, we design an optimal microgrid scheduling strategy based on typical day. In the day ahead operation cycle of the community microgrid, it maximizes the absorption of wind/solar unit outputs. This improves the operational efficiency of the microgrid and effectively reducing system operating costs. Extensive experiments demonstrate that the proposed model achieves superior performance compared with the original NSGA-III methods. The total daily operating costs of the proposed microgrid is reduced by 4.5%, and the renewable energy consumption rates is increased by 8.1%.

Keywords. Microgrid, NSGA-III, energy consumption, self-consistent energy system

1. Introduction

In the construction of smart cities, smart community microgrids, as important carriers of renewable energy, are facing two major challenges: firstly, the complex topology and dynamic operating environment of microgrids themselves; secondly, the intermittency and volatility of renewable energy output. In order to overcome these challenges, the integration of intelligent optimization control strategies is particularly important [1]. These strategies play a central role in the management of smart community microgrids. They not only enhance the reliability and stability of microgrids but also significantly reduce the economic operating costs of microgrids

¹ Corresponding Author: Lili PEI, peilili@chd.edu.cn.

through proactive system management and control measures. Intelligent control strategies accurately allocate energy resources, effectively balance load demands, and ensure the efficient and harmonious operation of smart community microgrids.

1.1. Related Work

Currently, scholars both domestically and internationally have conducted extensive research on the modeling and optimization scheduling strategies for multi-energy microgrids. Many researchers [2,3] have conducted studies on the synergistic operation between renewable energy and traditional energy sources. Exploring optimal matching strategies between energy storage technologies and various energy sources. Ma [4] proposes a coordinated scheduling model for wind power peak shaving and dissipation in an integrated energy system with multiple flexible devices. Kazda [5] proposes an optimal scheduling model that combines a closed-loop feedback controller with model predictive optimization (MPO). Wang [6] build a low-carbon economic dispatch strategy for an integrated energy system (IES). It concentrates on solar power (CSP) plants and established a framework for the low-carbon dispatch operation of the IES. However, the above studies primarily focus on addressing the supply and demand balance of single energy sources, ignoring the complementary of multiple energy sources and the economic feasibility in practical applications.

Hydrogen, as a new energy storage method [7], will greatly improve the utilization rate of electric energy during the enriched power generation periods when combined with wind/solar storage systems. Li [8] achieve rapid energy storage in hydrogen energy storage systems, by utilizing the rapid response of electrolyzers. Ganeshan [9] optimizes the wind/solar/hydrogen storage system with a certain communication base station as the load scenario. They take the maximum system load and minimum operating cost as the objective function. Verma [10] investigates the impact of different operating modes and partially cloudy weather conditions on hydrogen storage microgrid systems. Wang [11] proposes a comprehensive energy low-carbon economic dispatch model which combines wind power hydrogen production with various energy storage methods. This model optimizes the power output of each unit. Bosisio [12] investigates the feasibility of using green hydrogen generated through building-integrated photovoltaics to power off-grid housing. Emphasis on the size of the hydrogen storage tank, its year-round performance, and refueling to cope with hydrogen shortages. All of the aforementioned studies introduce hydrogen storage in hybrid energy systems. Most of their research focused on small-scale urban areas or experiments only under a single typical day. As a result, there are fewer studies on the optimal scheduling of integrated energy systems under large-scale or extreme weather conditions.

Optimal scheduling strategies are divided into two types: single-objective optimization and multi-objective optimization. Compared with the former, multi-objective optimization provides a favorable tradeoff between different performance indicators. Therefore, it is able to balance the conflicts between different objectives in the power system better. Anbarasan [13] conduct research on optimal energy management for microgrids utilizing renewable energy sources. They proposed a symbiotic organism search algorithm that simultaneously searches for multiple optimal solutions. It has strong local search capabilities. However, this algorithm faces challenges such as difficult parameter selection and high robustness requirements. Saleh [14] proposes a multi-objective optimization model that considers both the

operating costs of power plants and the cost of pollutant treatment in microgrids under grid-connected mode. However, this model suffers from slow convergence speed and long computation time. An optimization algorithm based on augmented electron constraints is established by Sun [15]. It implements the optimization search process by simulating the motion of particles in the electron cloud. However, the model is not effective in reducing the peak-to-valley difference of the grid and is highly dependent on the initial solution. Liu et al. [16,17] investigate the development of multi-objective optimization using genetic algorithms, focusing on two well-known algorithms: non-dominated sorting genetic algorithm (NSGA) and NSGA-II. The NSGA algorithm was proposed earlier, and its non-dominated sorting process has a high computational complexity, requiring a higher quality and diversity of the primary population. To further enhance the efficiency of the solution, NSGA-II employs a fast non-dominated sorting algorithm, an elite policy, and a non-dominated reservation mechanism. Improving the quality of the optimal solution while reducing time complexity has become the mainstream of multi-objective optimization algorithms. However, the issue of unevenly distributed solution sets and poor performance in optimization searches are apparent in practical applications.

1.2. Contributions

The main contributions of this paper are as follows:

- We introduce hydrogen energy storage, building a wind/solar/hydrogen storage microgrid systems. It converts surplus wind and solar energy into hydrogen during periods of abundant energy, which will be released during peak electricity demand for power supply. This strategy addresses the challenges of large and unstable fluctuations in renewable energy, enabling the system to adapt more flexibly to changes in electricity demand.
- We design the objective function to better optimize the scheduling of the proposed community microgrid system. Furthermore, we also design specific constraint conditions and search space for the objective function.
- We apply adaptive crossover and mutation strategy and fuzzy inference in NSGA-III algorithm. By utilizing the fuzzy inference mechanism, we dynamically adjust the algorithm parameters, solving the problem of that the algorithm itself has a slow convergence speed and the difficulty in finding high-quality solutions of NSGA-II. This improvement enhances the search efficiency and robustness of the NSGA-III algorithm.
- We design an optimal microgrid scheduling strategy based on typical day. In the day ahead operation cycle of the community microgrid, it maximizes the absorption of wind/solar unit outputs. This improves the operational efficiency of the microgrid and effectively reducing system operating costs.

The rest of this paper is organized as follows:

In Subsection I-A, we view some pertinent related work which may help the reader better understand this article. In Subsection I-B, we list the main contributions of this work. We build a mathematical model of wind/solar/hydrogen storage system in Section II. In Section III, We formally design a community microgrid day-ahead optimal scheduling model. In Section IV, we present the optimization algorithm based on improved NSGA-III. In Section V, we describe the datasets used, the parameters chosen for the algorithms, and the results obtained. We finally conclude in Section VI.

2. Wind/Solar/Hydrogen Storage Community Microgrid (WSH-SCM)

Urban community microgrids manifest distinctive regional attributes in energy distribution. For instance, in urban residential areas, such microgrids must account for the electricity demands of residential complexes, public amenities, and commercial enterprises. These locales invariably necessitate a dependable and unwavering power supply to cater to both daily life and business operations. Within urban settings, owing to dense infrastructure and spatial constraints, community microgrids can harness solar energy through the installation of photovoltaic panels on rooftops or available open areas, thereby converting it into usable electricity for communal consumption. Additionally, small-scale wind turbines can be erected in suburban or suitable open locales to generate electricity, seamlessly integrated into the community microgrid through grid connections.

With cities increasingly prioritizing sustainable development and ecological conservation, hydrogen energy is progressively acknowledged as a clean and renewable energy source. Consequently, community microgrids can explore the integration of hydrogen storage systems, which can store surplus wind and solar energy in the form of hydrogen gas generated via water electrolysis. This stored energy can then be utilized for fuel cell power generation, effectively balancing load demand and supply. Urban communities experience notable fluctuations in electricity demand during holidays, peak commuting hours, and extreme weather conditions such as hot summers and cold winters. In response to these challenges, community microgrids must adopt intelligent optimization control strategies to ensure efficient energy management and scheduling.

To cater to the specific requirements of urban communities, we have developed urban community microgrids incorporating wind, solar, and hydrogen storage capabilities. This approach not only enhances energy utilization efficiency but also diminishes reliance on conventional energy sources, thus fostering sustainable community development. Through the implementation of intelligent control strategies, these microgrids can operate reliably under diverse load conditions, thereby providing a dependable energy supply infrastructure for urban communities.

2.1. Structure of Wind/Solar/Hydrogen Storage Community Microgrid

The structure of the wind/solar/hydrogen storage community microgrid (WSH-SCM) is shown in Figure 1. It integrates all the typical controllable loads of the urban infrastructure in the community area. With the virtual power plant control technology, the photovoltaic output, wind turbine output, hydrogen storage, battery storage and electric vehicle charging stations are able to cooperate with each other. In this way, the day-ahead optimal schedule for the energy supply and load on a large scale is realized. The whole proposed microgrid contains three parts: energy supply, energy conversion and load energy consumption.

2.1.1. Energy supply

During the period of high concentration of new energy, wind, solar, and hydrogen energy sources are consumed to meet the electrical load demand of various systems. Surplus wind and solar power will first be stored in chemical batteries and electric vehicle charging stations. When the state of charge (SOC) of the battery reaches 100%, the remaining electrical energy is used to produce hydrogen through an electrolysis

device, which is then stored in a hydrogen storage tank. During off-peak hours of the external power grid, the energy supply part purchases electricity from outside. At peak load periods and low wind/solar output periods, this part will utilize the hydrogen in the storage tanks and the wind/solar units to supply power at the same time. When the supply of electrical energy is still insufficient, it purchases electricity from the external power grid.

2.1.2. Energy conversion

To fill the energy deficit caused by different time periods and load demands, we configure bi-directional energy storage devices in this part. They are composed of hydrogen storage tanks, battery packs, and electric vehicle charging stations. They store electricity during periods of surplus and discharge it during periods of deficit.

2.1.3. Load energy consumption

In urban community power service facilities, the power load comprises subsystems including monitoring systems, lighting systems, electric vehicle charging stations, service centers, et al.

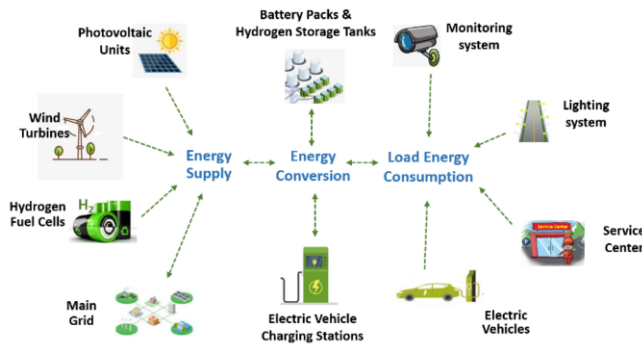


Figure 1. Overall framework of the proposed wind/solar/hydrogen storage community microgrid.

2.2. Mathematical Models for Power Output of Each Energy in WSH-SCM

2.2.1. Wind turbines generator

The output power of wind turbines generator (WTG) is closely related to the fluctuation of wind speed over time. According to [18], we use the probability density function of Weibull distribution to describe the day-ahead output power of wind turbines. The output power is calculated by the following equations:

$$f(v) = \frac{\mu}{\delta} v^{\left(\frac{\mu}{\delta}-1\right)} \left[\frac{\mu}{\Gamma\left(1+\frac{\mu}{\delta}\right)} \right]^{\frac{\mu}{\delta}} \exp \left[-\frac{v}{\mu} \right]^{\frac{\mu}{\delta}} \tag{1}$$

$$\varphi(v) = \frac{1}{\delta\sqrt{2\pi}} \exp \left[-\frac{(v-\mu)^2}{2\delta^2} \right] \tag{2}$$

$$P_w(v) = \begin{cases} \frac{P_r v}{v_r - v_{ci}} - \frac{P_r v_{ci}}{v_r - v_{ci}}, & v_{ci} < v < v_r \\ P_r, & v_r < v < v_\infty \\ 0, & v < v_{ci} \text{ or } v > v_\infty \end{cases} \quad (3)$$

Where v is the wind speed (m/s), $f(v)$ and $\varphi(v)$ refer to the probability density function and distribution function of wind speed, respectively. μ is the average wind speed and δ is the standard deviation. $\exp[\cdot]$ means exponential function. We obtain the output power $P_w(v)$ of wind turbines by equation (3). In this equation, P_r represents the rated output power. v_{ci} and v_r denote the cut-in wind speed and rated wind speed, respectively.

2.2.2. Photovoltaic unit

The output power of photovoltaic (PV) units depends on the total irradiance on the surface of the PV array at time t . It is a normal distribution. We utilize the following equation (4) to describe the relationship between the electrical energy produced by PV panels and the influencing factors such as solar irradiation intensity and temperature.

$$P_{PV}(t) = \frac{P_n G_t}{G_{ref}} f_\eta [1 + k(T_t - T_{ref})] \quad (4)$$

$P_{PV}(t)$ denotes the output power of the PV unit at time period t . The rated capacity of the photovoltaic panel is P_n . G_t and T_t are solar irradiation intensity and PV panel operating temperature, respectively. The reference irradiation intensity is G_{ref} and the reference operating temperature is T_{ref} . f_η means the operational efficiency of the photovoltaic units and k represents the temperature coefficient.

2.2.3. Main grid scheduling

A microgrid is a distributed energy system. When the generation power of the microgrid is less than the electrical load, the microgrid requires purchasing electricity from the main grid to fulfill the demand. When the power generated by the microgrid exceeds the electrical load, the microgrid sells the surplus electricity to the main grid and receives the corresponding revenue. The main grid scheduling model is expressed as the following equation:

$$P_{M,buy} + P_{M,sell} = P_{I,t} \quad (5)$$

Where $P_{M,buy}$ and $P_{M,sell}$ are purchased power and sold power, respectively. $P_{I,t}$ represents the power of the microgrid interacting with the main grid at time period t .

2.2.4. Hydrogen storage system

This system consists of hydrogen storage tanks, hydrogen supply devices, and fuel cell stacks. When there is an excess of electricity generated from renewable sources, the

surplus electricity is utilized to produce hydrogen, which is stored in the system. In case of peak load or insufficient wind/solar output, the hydrogen fuel cells will operate in conjunction with wind turbines and photovoltaic units to balance the difference between microgrid supply and demand. This ensures continuous power supply to the microgrid. The hydrogen storage systems improves the reliability and stability of microgrid by fully capitalizing on the excess production capacity of renewable energy sources and by providing back-up power support at times of peak demand on the grid. Its mathematical model and the expression for the capacity constraints of the hydrogen storage units are as follows:

$$L_{H_2}(t) = \frac{P_Q N_e}{VF} \tag{6}$$

$$P_Q(t) = L_{H_2}(t) \times C\eta \tag{7}$$

$$Q_{H_2}(t + \Delta t) = \int_{t_0}^{t_0 + \Delta t} L_{H_2}(t) dt + Q_{H_2}(t_0) \tag{8}$$

Where L_{H_2} is the rate of hydrogen consumption at moment t and P_Q is the output power of hydrogen fuel cells at moment t . P_Q denotes the rated capacity of one hydrogen fuel cell and N_e means the number of fuel cells in series. V and F represent voltage of the fuel cells and the Faraday's constant, respectively. C is the concentration of electrolyte. η is power generation efficiency of the system. Equation (8) refers to the quantity of hydrogen in hydrogen tanks at moment $t_0 + \Delta t$. It is obtained by summing both the initial amount Q_{H_2} at time t_0 and the consumption during Δt time period.

2.2.5. Electric vehicle charging station

We model the three states (standby, charging, and discharging) of an electric vehicle charging station as follows. In standby mode, the charging station has a load variation rate of 0. In the charging and discharging state, we take five factors that affects the load: the power and efficiency of charging, the power and efficiency of discharging, and the number of electric vehicles connected to the microgrid. The state of charge rate (SOC Rate) of electric vehicle charging station is calculated by equation (9) and equation (10).

$$SOC_c^k = \frac{P_c^k \eta_c^k}{Q^k} \tag{9}$$

$$SOC_f^k = \frac{-P_f^k}{\eta_f^k Q^k} \tag{10}$$

Where SOC_c^k and SOC_f^k denote the SOC Rate of charging and discharging, respectively. P_c^k , $-P_f^k$, and Q^k refer to the nominal charging power, the nominal discharging power and battery capacity for the k-type electric vehicles, respectively. The efficiency of charging is η_c^k and the efficiency of discharging is η_f^k .

3. Day-Ahead Optimal Scheduling of the Proposed WSH-SCM

The optimal scheduling model achieves the fully utilization and distribution of various energy sources within the microgrid. Considering constraints such as load balance, wind/solar outputs, and hydrogen storage, the problem of system resource allocation is formulated as a multi-objective optimization problem. Its objective function contains two components: the primary objective function and the secondary objective function. The constraints include wind/photovoltaic units output, primary grid output, hydrogen storage capacity, and storage battery power. We set the time interval of simulation to 1 hour. A more detailed description follows in the subsections below.

3.1. Primary Objective Function

We design a minimal total day-ahead operating cost as the primary objective function for the proposed WSH-SCM. It incorporates the cost of power supply from renewable energy sources, equipment maintenance costs, energy storage costs, and electricity transaction costs. The sum of them is the total intraday cost of our microgrid in 24 hours. The detailed formula for this main objective function is as follows:

$$\min C(t) = \sum_{t=1}^{24} (P_{W,t}C_W + P_{PV,t}C_{PV} + P_{Q,t}C_Q + P_{X,t}C_X + \beta + P_{M.buy,t}C_{b,t} - P_{M.sell,t}C_{s,t}) \quad (11)$$

Where C_W , C_{PV} , C_Q , and C_X refer to the unit operating cost of wind turbines, photovoltaic cells, hydrogen fuel cells, and storage batteries, respectively. $P_{W,t}$, $P_{PV,t}$, $P_{Q,t}$, $P_{M.buy,t}$ and $P_{M.sell,t}$ mean the relevant power value from equation (3) to equation (7) at time period t . The output power of the storage batteries at time period t is $P_{X,t}$. Furthermore, $C_{b,t}$ is the purchase price of electricity and $C_{s,t}$ denotes the sale price of that β means the total equipment maintenance cost per time period.

3.2. Secondary Objective Function

The secondary objective functions include three parts: load ratio, renewable energy consumption rate, and carbon emission.

3.2.1. Load ratio

Load ratio means the proportion of actual load power to maximum load power in the proposed community microgrid. The higher the load factor, the more utilization of the microgrid. However, when the load factor is too high, it will cause excessive load stress, which in turn affects the stability and reliability of the microgrid. Therefore, we need to increase the load ratio of the microgrid within a reasonable range according to our scheduling method. The formula of load ratio is described as follows:

$$\max LR(t) = \frac{1}{24} \sum_{t=1}^{24} \frac{P_{l,t}}{P_{\max}} \times 100\% \quad (12)$$

Where $P_{l,t}$ and P_{\max} are the actual load power to maximum load power at time period t , respectively.

3.2.2. Renewable energy consumption rate

This rate refers to the proportion of the actual power generation of renewable energy in the microgrid system to the total power supply. It reflects the sustainability of the microgrid and the efficiency of renewable energy utilization. We get it through the following method:

$$\max AR(t) = \sum_{t=1}^{24} \frac{P_{W,t} + P_{PV,t}}{P_{W,t} + P_{PV,t} + P_{M.buy}} \times 100\% \quad (13)$$

3.2.3. Carbon emission

To obtain the carbon emission of our microgrid, we first equate the main grid electricity generation to the amount of standard coal. Then we multiply it by the corresponding carbon emission factor. We adopt this part to evaluate the carbon emission level of different energy systems. The formula for calculating carbon emissions is as follows:

$$\min F(t) = \rho \sum_{t=1}^{24} \frac{P_{M.buy} \varpi}{\phi} \quad (14)$$

Where ρ is the carbon emission factor and it equals to 0.7476. ϖ denotes the coal consumption factor and its value is 0.45 kg/kWh. The calorific value of electricity generation is ϕ . It equals to 6300 kcal/kg.

3.3. Constraints

The constraints include four parts: wind/photovoltaic units output, primary grid output, hydrogen storage capacity, and storage battery power. In each unit time, the state of charge and the charging/discharging power of the equipments are required to satisfy constraints. Including electric power balance constraint, upper and lower bound constraint and unidirectional energy transfer constraint. We describe them in detail in the following content.

3.3.1. Wind/photovoltaic units output constraint

$$\begin{cases} P_{W,PV}(t) = 0, & \xi = 0 \\ \xi \Phi_{W,PV} \leq P_{W,PV}(t) \leq \xi P_{W,PV}^{\max}, & \xi = 1 \end{cases} \quad (15)$$

Where $\xi=0$ indicates the wind/photovoltaic unit equipment is off state, $\xi=1$ indicates unit equipment is on state; $\Phi_{W,PV}$ is the minimum load rate of equipment.

3.3.2. Primary grid output constraints

$$\begin{cases} 0 \leq P_{M.buy}(t) \leq P_{M.sell} \delta_{I,t1}, \\ P_{I\max} \delta_{I,t1} \leq P_{M.sell} \leq 0, \\ 0 \leq \delta_{I,t1} + \delta_{I,t2} \leq 1, \end{cases} \quad (16)$$

Where $\delta_{I,t1} + \delta_{I,t2}$ constraints limit transmission direction to unidirectional, ensuring the purchase and sale of electricity do not take place at the same time.

3.3.3. Hydrogen storage capacity constraints

$$\begin{cases} Q_{H_2}^{\min} \leq Q_{H_2}^t \leq Q_{H_2}^{\max}, \\ Q_{H_2}^0 = Q_{H_2}^{24}, \end{cases} \quad (17)$$

Where $Q_{H_2}^0 = Q_{H_2}^{24}$ indicates the energy storage capacity remains unchanged before and after optimal scheduling; $Q_{H_2}^{\max}$ and $Q_{H_2}^{\min}$ are the upper and lower limits of hydrogen storage tank capacity.

3.3.4. Storage battery power constraints

$$P_{W,v} + P_{PV,t} + P_{M,t} + P_{Q,t} + P_{X,f} = P_{L,t} + P_{X,c} \quad (18)$$

$$\begin{cases} SOC_{\min} \leq SOC_t \leq SOC_{\max}, \\ 0 \leq P'_{X,f} \leq (1 - \tau_t) P_{X,f}^{\max}, \\ 0 \leq P'_{X,c} \leq \tau_t P_{X,c}^{\max}, \end{cases} \quad (19)$$

Where P_L is the microgrid load power; $P_{X,c}$ and $P_{X,f}$ are the battery charging/discharging power, respectively, and the upper limit is P_X^{\max} ; SOC_{\max} and SOC_{\min} are the upper and lower limits of battery charge of state; τ_t is a variable between 0 and 1, restricts the energy storage device can only unidirectional energy transfer at time period t .

4. Improved Nsga-III Application in WSH-SHM

4.1. Improved NSGA-III Algorithm

4.1.1. Adaptive mechanism-based population crossover and mutation strategy

Crossover and mutation are the primary operations for global and local search in the NSGA-III algorithm, exerting significant influence on the overall performance of the algorithm. The crossover operation involves recombining partial genes of each individual in the population to achieve global exploration. The mutation operation involves randomly modifying a portion of genes in individual populations to achieve local exploration and increase population diversity. Similar to many evolutionary algorithms, NSGA-III faces challenges in exploring different regions of the solution space and developing the Pareto front set. To overcome these challenges, adaptive crossover and mutation strategies have been introduced.

We dynamically adjust the crossover and mutation operators based on the fitness function (see Equation 20 and 21). This effectively addresses the issue of low optimization efficiency. P_{ac} refers to the adaptive crossover probability and P_{am} represents the mutation probability. The adaptive crossover and mutation strategy is able to dynamically adjust the crossover and mutation rates while selecting superior individuals. This ensures that only the most suitable individuals participate in crossover and mutation operations (shown in Figure2). The optimal gene segments in the

population are effectively retained and passed to the next generation. This adaptability improve convergence speed and prevents premature convergence to sub-optimal solutions. In addition, these improvements are particularly advantageous for escaping local optima and maintaining population diversity. They enable the algorithm to find high-quality solutions for complex, dynamic, and diverse optimization problems, imparting greater robustness.

$$P_{ac} = \begin{cases} \frac{\alpha_1(f_{\max} - f_c)}{\cos(\frac{f_{avg} - f_{\max}}{f_{avg} - f_{\min}})}, & f_c \geq f_{avg} \\ 1 + e^{\frac{f_{avg} - f_{\max}}{f_{avg} - f_{\min}}}, & f_c < f_{avg} \end{cases} \quad (20)$$

$$P_{am} = \begin{cases} \frac{\alpha_3(f_{\max} - f_m)}{\cos(\frac{f_{avg} - f_{\max}}{f_{avg} - f_{\min}})}, & f_m \geq f_{avg} \\ 1 + e^{\frac{f_{avg} - f_{\max}}{f_{avg} - f_{\min}}}, & f_m < f_{avg} \end{cases} \quad (21)$$

Where f_{\max} , f_{\min} indicates the maximum and minimum fitness values in the population. f_c is the larger fitness value of the two individuals to be crossed, f_m is the fitness value of the individual to be mutated, f_{avg} is the average fitness value of the population. The parameter α_{1-4} , indicates crossover and mutation probability control coefficient.

To enhance adaptive efficiency, in the early stages of the algorithm, larger mutation rates and smaller crossover rates are employed to facilitate rapid exploration across the global solution space. As the algorithm progresses, the mutation rate decreases, and the crossover rate increases, facilitating better escape from local optima and generating a greater number of new individuals. Besides, this study integrates the non-dominance ranking of crossover and mutation targets in different evolutionary stages, providing a more detailed reflection of the population's evolutionary progress. This effectively enhances the algorithm's global and local search capabilities.

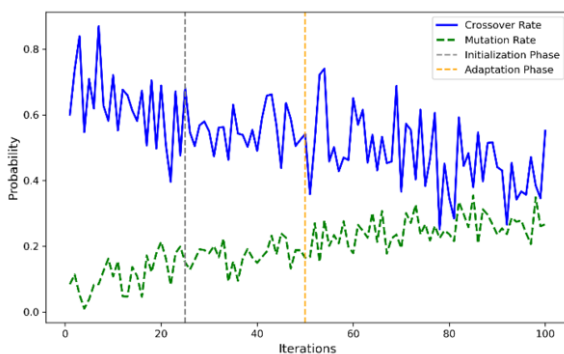


Figure 2. Adaptive crossover versus variance probability change plots

4.1.2. Improved fuzzy inference-based NSGA-III for multi-objective optimization

In multi-objective setting, NSGA-III ranks individuals in the population based on their non-dominance levels. The ranking process is accomplished through selection, crossover, and mutation operations. However, during the optimization process, a large number of

non-dominated solutions are generated, leading to the model's inability to adequately fit the features in the training set.

To address this issue, we introduce fuzzy similarity theory to perform attribute reduction on the parameters of controllable power load data, obtaining a more effective feature set. Subsequently, we address the underfitting issue by iteratively updating the population center and membership relationships. The formulas for fuzzy lower approximation membership and fuzzy upper approximation membership of the objective function are as follows:

$$\begin{cases} x_{pix}(H_i) = \inf_y \max\{1 - H_{ix}(y), x_H(y)\}, \forall_i \\ x_{psx}(H_i) = \sup_y \min\{H_{ix}(y), x_H(y)\}, \forall_i \end{cases} \quad (22)$$

Where H_i represents the fuzzy equivalence classes between the universe of discourse (U) and conditional attributes. It ensures data elements in each subset have a similar degree of affiliation. \inf and \sup are mean to take the minimum and maximum values in operation. The variables x and y both represent samples; $1 - H_{ix}(y)$ indicates the inverse of the sample's affiliation to the equivalence class H_i .

The fuzzy-rough operator is established on the foundation of the fuzzy lower approximation concept, to optimize and filter the attributes in data. The union of lower approximation sets is defined as the positive region of the rough set. The membership degree formula for the fuzzy positive region is as follows:

$$x_{posp}(t) = \sup_{H_i} \min[x_{ix}(y), x_{posp}(H_i)], \forall_i \quad (23)$$

$$\lambda_k(Q) = \frac{|x_{posp}(y)|}{|x|} = \frac{\sum x_{posp}(y)}{|x|} \quad (24)$$

Where x_{posp} indicates the membership functions in fuzzy domains; λ_k indicates the dependency function of conditional attributes on the decision attribute Q .

Through determining the Pareto optimality bound, the improved NSGA-III multi-objective optimization algorithm is able to solve the trade-off problem between multiple objective functions. It considers not only a single locally optimal solution, but also the relationship between multiple solutions.

4.2. Microgrid Optimal Scheduling Process

In this paper, we utilize the Long Short-Term Memory (LSTM) algorithm [19] for multi-step forecasting firstly, focusing on the effective prediction of the power generation from wind/solar units in the short term for day-ahead. Furthermore, we analyze the load data samples collected from different types of electrical systems, and restructure the data to simulate load demands under extreme hot, extreme cold, and normal climatic conditions. Secondly, we establish a multi-objective optimization model for a wind/solar/hydrogen storage microgrid based on the objective function and constraint conditions. Using improved NSGA-III algorithm to solve the multi-objective optimization. The flow chart of microgrid optimal scheduling algorithm based on the improved NSGA-III is shown in Figure 3.

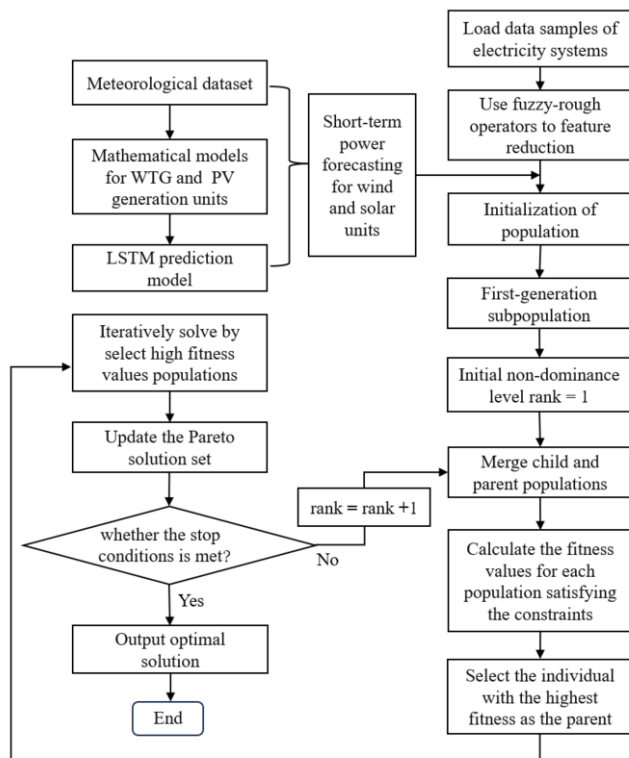


Figure 3. Flowchart of improved NSGA-III algorithm.

5. Example and Simulation Verification

5.1. Example Description

The integrated Community Comprehensive Self-Consistent Energy System structure employed in this study is illustrated in Figure1. It incorporates distributed energy sources such as photovoltaics, wind turbines, and energy storage devices, while simultaneously addressing various load demands including cooling, heating, and electricity.

The study focuses on a summer typical day in a certain urban community. The community microgrid load system consist of monitoring system, communication system, lighting system, service life system, and energy storage regulation system. Assuming that both the electrical load system and energy storage regulation system within the microgrid participate in the optimization scheduling, the specific equipment parameters involved in WSH-SCM are detailed in Table 1.

Simulating based on the daily electricity consumption pattern at the community area, the energy consumption data for typical day cooling, heating, and electricity loads are obtained, as shown in Figure4. Utilizing existing short-term forecasting methods for wind and solar power, the variation curves for wind turbines and photovoltaics are obtained as shown in Figure5. The daily electricity price adopts a time-of-use pricing

structure, with off-peak hours from 0:00-6:00, standard hours from 6:00-9:00, 15:00-18:00, and 20:00-24:00, and peak hours from 9:00-15:00 and 18:00-20:00, as illustrated in Figure6. The microgrid is set to allow a maximum load shedding rate of 3%, with the maximum charge/discharge power within a unit of time not exceeding 30% of the energy storage capacity. The allowable power exchange between the microgrid and the main grid is restricted to not exceed 150 kW.

Table 1. Simulation parameter table for WSH-SCM.

Regulation project	Parameter	Value
Electric vehicle charging station	rated power/kW	13
	charge/discharge efficiency	0.87
	unit capacity/kWh	15
	operating cost ¥/kWh	0.6
Storage battery constraints	rated power/kW	3.7
	charge/discharge efficiency	0.97
	unit capacity/kWh	3.8
	operating cost ¥/kWh	0.18
Hydrogen fuel cell	rated power/kW	8
	charge/discharge efficiency	0.4
	unit capacity/kWh	20
Hydrogen storage tank	operating cost ¥/kWh	0.7
	unit capacity/L	40
Wind turbines generator	Acquisition cost ¥/pc	500
	unit capacity/kWh	1.7
Photovoltaic units	operating cost ¥/kWh	0.52
	unit capacity/kWh	200
	operating cost ¥/kWh	0.75

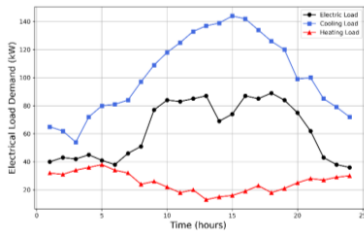


Figure 4. Intraday variation curves for each type of energy load.

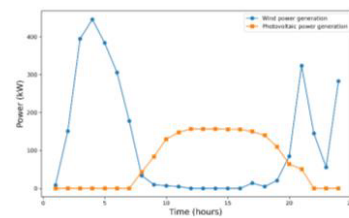


Figure 5. Intraday variation curves for wind and solar power generation.

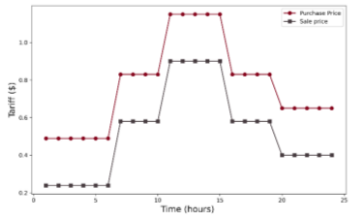


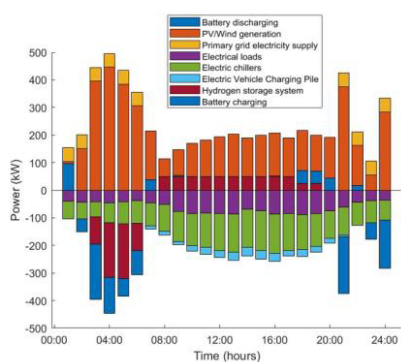
Figure 6. Time-sharing tariff

5.2. Simulation Result Analysis

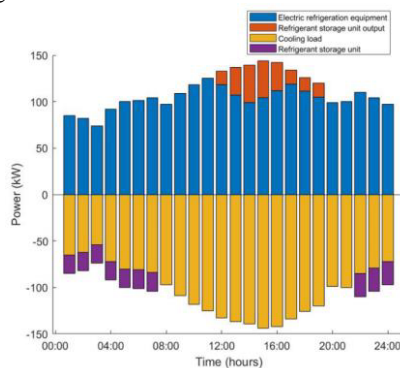
This paper conducts simulation and emulation of WSH-SCM, employing the improved NSGA-III multi-objective optimization algorithm for optimized scheduling. The obtained configuration results are presented in Table 2. With this configuration, the

microgrid achieves electrical balance (as shown in Figure 7.), maintaining a stable operational state, and minimizing the total daily operational cost.

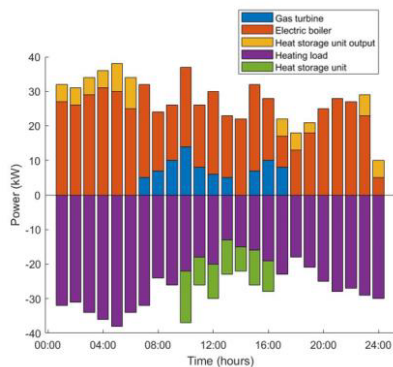
In terms of electrical load, wind and solar power generation serve as the main power supply throughout the entire timeframe, ensuring continuous power supply. During off-peak electricity pricing periods (0:00–6:00 and 21:00–24:00), WSH-SHM procures a substantial amount of electricity, charges energy storage devices, and utilizes externally purchased electricity to produce and store hydrogen. In contrast, during peak electricity pricing periods (10:00–15:00 and 19:00–20:00), the gas turbine generator provides auxiliary power, and energy storage devices discharge. As for the cooling load, the electric chiller operates efficiently throughout the entire timeframe, particularly during peak electricity pricing periods (8:00–18:00). The absorption chiller provides additional cooling support, and the cold storage unit discharges cold energy. For the thermal load, during off-peak electricity pricing periods, the electric boiler provides heating, and the thermal storage unit stores heat. Meanwhile, during peak electricity pricing periods, the gas turbine takes on the heating task, with the thermal storage unit releasing heat and providing auxiliary heating.



(a) Electrical load and each equipment module output power.



(b) Cooling load and refrigeration equipment output power.



(c) Thermal load and equipment output power.

Figure 7. Intraday variation curves for wind and solar power generation.

To validate the practicality of the improved NSGA-III, this study compares the proposed algorithm with simulated annealing particle swarm optimization algorithm (SA-PSO), NSGA-II algorithm, and the original NSGA-III algorithm in the optimization scheduling problem of WSH-SHM through comparative experiments. The

specific parameter settings and experimental results are presented in Table 3. It can be observed that the improved NSGA-III algorithm exhibits a significant advantage in convergence speed. At the same population size, the average convergence times for the four algorithms are 1.07 s, 1.27 s, 0.94 s and 0.87 s, respectively. Compared to the original NSGA-III algorithm, it achieves speedup rates of 18.69%, 31.50%, and 7.45%, respectively. In terms of the number of iterations required for the algorithm to converge, the SA-PSO algorithm converges around the 275th generation, the NSGA-II algorithm achieves the optimal solution only at the 300th generation, the original NSGA-III algorithm reaches an ideal value around the 230th generation, while the fuzzy inference-based NSGA-III algorithm, benefiting from the improved quality of the initial solution, attains the ideal value around the 200th generation. Compared to the other three algorithms, the proposed algorithm consistently obtains superior solutions.

Table 2. Simulation parameter table for WSH-SCM.

Equipment project	Value
Electric vehicle charging station	42
Storage battery constraints	56
Hydrogen fuel cell	11
40L Hydrogen storage tank	18
Wind turbines generator	4
Photovoltaic units	64
Electric refrigeration equipment	20
Gas turbine	3
Electric boiler	2

Table 3. Comparison of Algorithmic Solution Instances.

Parameters	SA-PSO	NSGA-II	NSGA-III	Improved NSGA-III
Population Size	200	200	200	200
Iteration Number	275	300	230	200
Convergence Time/s	1.07	1.27	0.94	0.87
Total Cost/¥	1754.10	1747.50	1671.20	1596.07
Load Ratio	75.3%	71.5%	82.3%	75.1%
Consumption Rate	65.5%	78.8%	74.5%	82.6%
Carbon Emission/t	0.071	0.046	0.050	0.034

In summary, the fuzzy inference-based NSGA-III algorithm designed in this study exhibits superior stability. Making significant progress in improving the quality of the initial solution and reducing the convergence time of the algorithm. It achieves convergence with fewer iterations. Furthermore, this algorithm contributes to minimizing the overall operational cost of the community microgrid system (WSH-SCM), increasing the renewable energy integration rate, and exhibiting superior global search capabilities. It effectively avoids local minima, adapts well to the uncertainty of wind and solar outputs, and meets real-time requirements, resulting in reasonable optimized scheduling plans.

6. Conclusion

This paper addresses the issues related to energy supply and demand management and the utilization of renewable energy in urban smart community microgrid. Firstly, we

introduce hydrogen energy storage and establish the WSH-SCM system to maximize the absorbed wind/solar unit output while power peak-filling during the daily operation cycle of the microgrid. Secondly, in order to realize the day ahead optimal scheduling of the community microgrid more effectively, we design a special objective function and constraints for the system to complete the mathematical modeling. Thirdly, we improve the NSGA-III algorithm by applying adaptive crossover and mutation strategy and fuzzy inference, which solve the problem that the algorithm itself has a slow convergence speed and poor globally optimal solution. This enhances the adaptability of the algorithm to the uncertainty of source load variation. The improved NSGA-III provides better optimal scheduling solution for the WSH-SCM system.

The experiment results indicate that the proposed algorithm in this paper performs outstandingly in maintaining population diversity and convergence. It brings a significantly improved optimization scheduling effect. The algorithm provides a feasible and efficient solution to address the multi-objective optimization problem of resource allocation. In the subsequent research, further exploration will be conducted to design various fuzzy systems for parameter adjustment, aiming to address optimization scheduling problems in multiple urban scenarios.

References

- [1] Yuping Zhang, Youyang Qu, Longxiang Gao, Tom Hao Luan, Alireza Jolfaei, James Xi Zheng, "Privacy-preserving data analytics for smart decision-making energy systems in sustainable smart community," *Sustainable Energy Technologies and Assessments*, Volume 57, 2023, 103144, ISSN 2213-1388, <https://doi.org/10.1016/j.seta.2023.103144>.
- [2] Y. Zhang, F. Wu, K. Lin, L. Shi, Y. Li and Y. Bao, "Optimal Dispatching Strategy for Concentrating Solar Power Plant to Suppress Output Power Fluctuation of Wind-photovoltaic System," 2021 IEEE 4th International Electrical and Energy Conference (CIEEC), Wuhan, China, 2021, pp. 1-5, doi: 10.1109/CIEEC50170.2021.9510328.
- [3] H. Zhu, H. H. Goh, T. Liu, H. Dai, D. Zhang and T. Wu, "Intelligent Path Modeling for Large-Scale Multi-energy Microgrid Considering Demand-side Management," 2021 5th Asian Conference on Artificial Intelligence Technology (ACAIT), Haikou, China, 2021, pp. 600-605, doi: 10.1109/ACAIT53529.2021.9731245.
- [4] Z. Ma, J. Zhang, S. Liu and H. Dong, "Optimal Scheduling Method of Wind Power-photovoltaic-photothermal Integrated Energy System with Flexibility in Mind," 2022 IEEE 5th International Electrical and Energy Conference (CIEEC), Nanjing, China, 2022, pp. 4277-4282, doi: 10.1109/CIEEC54735.2022.9846255.
- [5] J. Kazda and N. A. Cutululis, "Model-Optimized Dispatch for Closed-Loop Power Control of Waked Wind Farms," in *IEEE Transactions on Control Systems Technology*, vol. 28, no. 5, pp. 2029-2036, Sept. 2020, doi: 10.1109/TCST.2019.2923779.
- [6] Z. Wang, X. Zhang, X. Zhang and S. Huang, "Low-carbon Optimal Dispatch of Integrated Energy System Considering Concentrating Solar Plant," 2022 IEEE/IAS Industrial and Commercial Power System Asia (I&CPS Asia), Shanghai, China, 2022, pp. 1239-1244, doi: 10.1109/ICPSAsia55496.2022.9949692.
- [7] A. Ghezelbash, V. Khaligh, J. Liu and J. -H. Ryu, "Scheduling of a Multi-energy Microgrid Enhanced with Hydrogen Storage," 2022 IEEE PES 14th Asia-Pacific Power and Energy Engineering Conference (APPEEC), Melbourne, Australia, 2022, pp. 1-6, doi: 10.1109/APPEEC53445.2022.10072138.
- [8] Q. Li, X. Zou, Y. Pu and W. Chen, "A Real-time Energy Management Method For Electric-hydrogen Hybrid Energy Storage Microgrid Based on DP-MPC," in *CSEE Journal of Power and Energy Systems*, doi: 10.17775/CSEEJPES.2020.02160.
- [9] A. Ganeshan, D. G. Holmes, L. Meegahapola and B. P. McGrath, "Enhanced Control of a Hydrogen Energy Storage System In A Microgrid," 2017 Australasian Universities Power Engineering Conference (AUPEC), Melbourne, VIC, Australia, 2017, pp. 1-6, doi: 10.1109/AUPEC.2017.8282434.

- [10] Verma S. "Effect of Hysteresis Band Control Strategy on Energy Efficiency and Durability of Solar-Hydrogen Storage Based Microgrid in Partial Cloudy Condition" *The Journal of Energy Storage*, 2020, 32. DOI:10.1016/j.est.2020.101936.
- [11] G. Wang, H. Fan, M. Bi, C. Huang, Y. Fan and C. Liu, "Considering Low-Carbon Economic Dispatch of Power Systems with the Participation of Large-Scale Energy Storage and Multiple Types of Regulation Resources," 2023 5th Asia Energy and Electrical Engineering Symposium (AEEES), Chengdu, China, 2023, pp. 1423-1428, doi: 10.1109/AEEES56888.2023.10114252.
- [12] A. Bosisio, A. Morotti, S. Penati, A. Berizzi, C. Pasetti and G. Iannarelli, "A Feasibility Study of Using Renewable Based Hydrogen in Off-grid Domestic Energy Systems: A Case Study in Italy," 2022 Second International Conference on Sustainable Mobility Applications, Renewables and Technology (SMART), Cassino, Italy, 2022, pp. 1-7, doi: 10.1109/SMART55236.2022.9990178.
- [13] P. Anbarasan and T. Jayabarathi, "Optimal Reactive Power Dispatch Problem Solved by Symbiotic Organism Search Algorithm," 2017 Innovations in Power and Advanced Computing Technologies (i-PACT), Vellore, India, 2017, pp. 1-8, doi: 10.1109/IPACT.2017.8244970.
- [14] M. Saleh, Y. Esa, N. Onuorah and A. A. Mohamed, "Optimal Microgrids Placement in Electric Distribution Systems Using Complex Network Framework," 2017 IEEE 6th International Conference on Renewable Energy Research and Applications (ICRERA), San Diego, CA, USA, 2017, pp. 1036-1040, doi: 10.1109/ICRERA.2017.8191215.
- [15] Z. Sun et al., "An Evolutionary Algorithm With Constraint Relaxation Strategy for Highly Constrained Multiobjective Optimization," in *IEEE Transactions on Cybernetics*, vol. 53, no. 5, pp. 3190-3204, May 2023, doi: 10.1109/TCYB.2022.3151974.
- [16] Y. Liu, G. Cheng and J. Zhu, "Multi-Objective Non-Cooperative Game Optimization for Microgrid Clusters Based on NSGA-II Coordinated Interior-Point Method," 2021 IEEE Power Energy Society General Meeting (PESGM), Washington, DC, USA, 2021, pp. 1-5, doi: 10.1109/PESGM46819.2021.9638127.
- [17] Jingrui Zhang, Junfeng Cai, Hongcai Zhang, Tengpeng Chen, "NSGA-III Integrating Eliminating Strategy and Dynamic Constraint Relaxation Mechanism to Solve Many-objective Optimal Power Flow Problem", *Applied Soft Computing*, Volume 146,2023,110612,ISSN 1568-4946,https://doi.org/10.1016/j.asoc.2023.110612.
- [18] Q. Zhang, X. Chen, G. Li, J. Feng and A. Yang, "Model Predictive Control Method of Multi-Energy Flow System Considering Wind Power Consumption," in *IEEE Access*, vol. 11, pp. 86697-86710, 2023, doi: 10.1109/ACCESS.2023.3304697.
- [19] K. Moharm, M. Eltahan and E. Elsaadany, "Wind Speed Forecast using LSTM and Bi-LSTM Algorithms over Gabal El-Zayt Wind Farm," 2020 International Conference on Smart Grids and Energy Systems (SGES), Perth, Australia, 2020, pp. 922-927, doi: 10.1109/SGES51519.2020.00169.